BETA-GALACTOSIDASE FROM PSYCHROTROPHIC MICROORGANISM (STRAIN ARTHROBACTER)

J. Hašek[1], T. Skálová[1], H. Petroková[1], E. Buchtelová[1], J. Dohnálek[1], V. Spiwok[2], P. Lipovová[2], H. Strnad[2] and B. Králová[2]

[1]Institute of Macromolecular Chemistry, Academy of Sciences of the Czech Republic, Heyrovského nám. 2, 162 06 Praha 6, Czech Republic
[2]Institute of Chemical Technology, Technická 5, 166 28 Praha 6, Czech Republic

Keywords:
ß-galactosidase, cold active enzymes, *Arthrobacter*, protein crystallography, molecular modeling,

Abstract
The cold active ß-galactosidase isolated from *Arthrobacter* sp. C2-2 was expressed and fully characterized. The diffraction measurements were completed and the 3D structure determination is in progress. Comparison of preliminary structure shows that the enzymes from psychrophilic and thermophilic organisms have high conformation similarity in spite of homology 32 % only. A role of mutations important for activity and the conformational stability of the enzyme are analyzed by energy calculations.

Introduction

The ß-galactosidase from Arthrobacter sp. C2-2, main subject of this study, was derived from bacteria living in Antarctica under low temperatures (permanently below 5 °C). Its low temperature activity deserves special attention because of many practical and theoretical impacts of enzymatic processes under ambient temperatures [1, 2]. The elucidation of low temperature adaptation of enzymes requires knowledge of detailed molecular geometry and an analysis of conformational changes in the active site. The only known method being able to give complete determination of structure of large proteins is the X-ray crystallography. Therefore, the first part of our project is to determine the structure the above mentioned cold-active enzyme using X-ray diffraction.

Structure determination

Cold active ß-galactosidase from Arthrobacter sp. C2-2 is a large protein homological to the ß-galactosidase from Escherichia coli (sequence identity 32%). The details concerning the expression, purification and determination of basic characteristics of the protein performed in the Institute of Chemical Technology in Praha were published in [1, 2].

The protein was crystallized using hanging drop method. Crystallization drops contained 1 µl protein solution and 1 µl reservoir solution. Protein solution: 4 mg/ml in 10 mM potassium phosphate buffer pH 7.5, 1 mM $MgSO_4$, 1 mM NaN_3 . Reservoir solution: 20% PEG 4000, 200 mM NaCl, 200 mM ammonium sulphate in 100 mM Na citrate buffer, pH 5.6. The final crystals were obtained by microseeding, i.e. doping the crystallization drop by several microcrystals obtained in preliminary crystallization attempts. The crystal was soaked in the mother liquor with 20 % ethylene glycol shortly before measu-rement.

In spite of large and optically perfect crystals, the successful X-ray diffraction measurement required high intensity of primary X-ray beam. The final measurement was performed at the source of synchrotron radiation ESRF in Grenoble at the beam line ID 29. Because of large unit cell (a = 140.1, b = 205.7, c = 140.5 Å, ß = 102.3°, space group $P2_1$), the diffraction data was collected with small oscillation angle 0.1°. Total 1800 frames gave 28 millions of measurements up to resolution 1.9 Å. They were processed by special version of the HKL package of programs [3] for viruses. All data processed up to 1.9 Å gave 579289 unique reflections, R_{lin} = 8.5 % and completeness 95 %.

The phase problem was solved by the program EPMR (molecular replacement by evolutionary search [4]) using the structure of ß-galactosidase from *Escherichia coli* (PDB code 1DP0, resolution 1.7 Å) as a model [5]. In spite of low homology, the global structure of one monomer unit appears similar. The structure building of the protease tetramer into the maps of electron density and the refinement is under progress.

The Fig. 1 shows a cartoon-view of a monomer of the ß-galactosidase from Arthrobacter sp. C2-2 obtained by homology modeling using program Modeler [6] starting from the ß-galactosidase from *Escherichia coli* (homology ~30 %). Conformations of side chains of the Glu442 and Glu521 in the active site of ß-galactosidase are shown in stick and ball model.

Conclusion

The x-ray structure determination using synchrotron radiation provides a reliable and sufficiently exact experimental view of the molecular structure even in the case of large protein macromolecule like this structure. This information gives a complete geometrical view on binding and mobility of the products, intermediate products and substrates (measured after slight mutation of the active site) which is necessary for a reliable description of the enzymatic process. The mutation experiments and research of ß-galactosidase complexes necessary for a reliable interpretation of low temperature activity of ß-galactosidase from psychrotrophic microorganism Arthrobacter sp. C2-2 are under way.

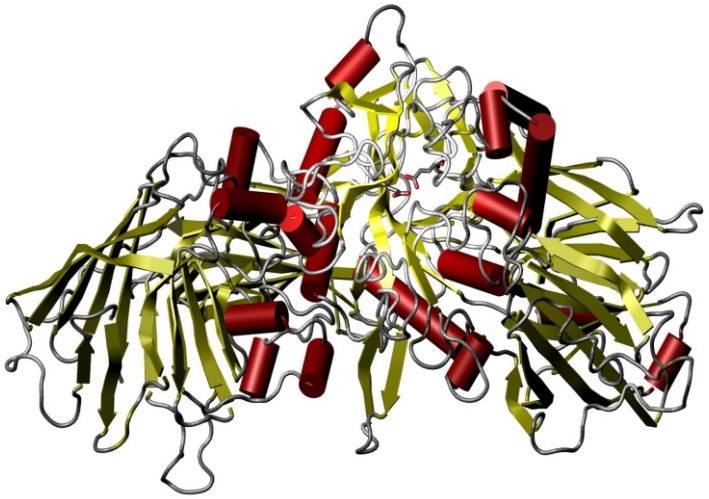

Figure 1. Monomer of ß-galactosidase from psychrotrophic microorganism Arthrobacter sp. C2-2 living in Antarctica under low temperature.

Acknowledgment
The research is supported by the Grant Agency of the Czech Republic (project 204/02/0843/A) and by the Academy of Sciences of the Czech Republic (project AVOZ4050913).

References

1. P. Karasová, V. Spiwok, Š. Malá, B. Králová, N. J. Russell, *Czech J. Food Sci.* (2002) 43-47.
2. P. Karasová-Lipovová, H. Strnad, V. Spiwok , Š. Malá, B. Králová, N.J. Russell, *Enzyme Microb. Tech.* (2003) 836-844.
3. Z. Otwinowski and W. Minor, Methods in Enzymology: *Macromolecular Crystallography* **A276** (1997) 307-326.
4. C.R. Kissinger, K. D.K. Gehlhaar, B.A. Smith, EPMR - A program for crystallographic molecular replacement by evolutionary search. Version 2.5. Agouron Pharmaceuticals, Inc, http://www.msg.ucsf.edu/local/programs/epmr/epmr.html.
5. Juers, D. H., Jacobson, R. H., Wigley, D., Zhang, X. J., Huber, R. E., Tronrud, D. E., Matthews, B. W., *Protein Sci.* **9** (2000) 1685-1699.
6. Šali A., Blundell T., Comparative protein modelling by satisfaction of spatial restraints. *J. Mol. Biol*. **234** (1993) 779-815.

SOME RECENT NON-TRADITIONAL APPLICATIONS OF X-RAY SCATTERING TECHNIQUES IN BIOLOGY

Radomír Kužel

Faculty of Mathematics and Physics, Charles University, 121 16 Praha 2, Ke Karlovu 5

Keywords
powder diffraction, X-ray reflectivity, grazing incidence, standing waves, membrane structure

Abstract
Some recent applications of powder diffraction in biology are shortly reviewed. Not only structure refinement of proteins from powder data obtained by high-resolution synchrotron but also investigations of real structure of biological materials like wood. Other examples are mentioned from studies of biological membranes by X-ray reflectivity, grazing incidence and standing waves.

1. Introduction

In the last decade, single crystal X-ray diffraction has become a routine and well-known technique of protein structure analysis. Synchrotron radiation is often required and preparation of suitable single crystals may be not so easy.

However, this is not the only use of X-ray diffraction and X-ray scattering in biology. In this short review, several other examples will be mentioned - powder diffraction, X-ray reflectivity, grazing incidence, standing waves. These techniques are mainly used for structural investigations of biological membranes.

2. Powder diffraction

In last years, *structure refinement* and even *structure determination* from powder diffraction has become more and more popular. This has been routinely used in chemistry, physics and also materials science. For large molecules it is rather complicated because the information in powder pattern is much lower than in full single-crystal pattern (actually one-dimensional projection) and moreover, huge number of diffraction lines leads to their strong overlap. However, recently successful attempts of protein structure refinement have been performed due to fast development in instrumental techniques, namely high-resolution diffraction with synchrotron radiation. Pioneer work was presented by von Dreele [1, 2] and it started series of other experiments, especially at ESRF high-resolution beamline [e.g. 3a, 3b]. Other experiments were performed in Japanese synchrotron SPring8, Brookhaven National Laboratory (NSLS) and in Argonne National Laboratory. Different proteins were studied - lysozymes, ribonuclease, myoglobin, bovine insulin, trypsines. Even the lifetime of the samples at room temperature may be not very long (e.g. 2 minutes), it is sufficient for collection of high-quality patterns. The lifetime can be increased at lower temperatures but it has also been found that the quality of powder can often been deteriorated at low temperatures. Phase changes can appear at low temperatures.

Current molecular weight limit is moving from 50 kDa to 100 kDa. There is stil no present way of solving protein structures *ab initio* from powder data, but model building and molecular replacement work quite well. The combination of Rietveld- and stereochemical/restraint refinement has been proposed.

Experiments have also shown how powerful powder diffraction can be for *investigations of protein structure variations with changes of external conditions*. High-resolution powder diffraction patterns can display considerable sensitivity to subtle structural changes which can be seen in peak shifts, broadening and intensity changes. Protein lattice parameters determined from powder data are up to two orders of magnitude more precise than that obtained from typical single-crystal experiments. Distinct advantages of powder diffraction can also be its complete immunity to crystal fracture and to any phase change that may accompany complex formation.

Of course, the biological applications of powder diffraction are not restricted only to proteins. Inorganic, mineral parts of biological objects can be investigated as-well. One example has been shown in preceding Meeting of the Czech and Slovak Structural Biologists [5]. Other can be found for example in [6].

Investigation of wood belongs to another interesting biological application of powder diffraction. Recently, its stress-strain curves were analysed with synchrotron radiation [7] where individual wood cells could be measured and compared with the results obtained from thin wood foils. The deformation process is explained by stick-slip mechanism at molecular level which plays a role of dislocation gliding in metals. It was found that there is molecular recovery in the cell wall. The wood texture and its change with the strain was investigated as well.

Similar techniques to powder diffraction are usually used for *fibre diffraction*. The method has its own Web site on Fibre Diffraction and Polymer Diffraction [8]. It is used for example for study of muscles [9-12].

3. X-ray scattering on surfaces and thin films

3.1 X-ray reflectivity and grazing-incidence diffraction

Interest in X-ray investigations of surface layers, thin films and multilayers has increased dramatically during last decadee. In addition to traditional diffraction techniques - both single crystal and powder diffraction, new methods have been developed: X-ray reflection, grazing incidence diffraction and X-ray standing waves. Several review and tutorial papers on these techniques were published in this journal [13-17]. (Illustrations below are taken from these references). There are also monographies devoted to the problem [e.g. 18].

The methods found their applications especially in physics, microelectronics, optics, technology etc. Also some biological applications appeared and their number is increasing in last years. Namely for study of biological membranes.

What is the principle and what we can learn? For the complete description of the scattering phenomena dynamical theory must be used.

The pecularity of the electromagnetic waves in the X-ray region is that the refractive index of real materials is less than unity as the electromagnetic transitions within the atoms are excited. Therefore, the effect of *total reflection* of X-rays occurs below the critical angle of incidence ($_c$), see Fig. 1, E_s. Refraction index can be written in the form

$$n \quad 1 \qquad i$$

with

$$\frac{}{2} r_e \quad _e ; \qquad \frac{}{4} \quad _x$$

$r_e = 2.818 \quad 10^{-15}$ m is the classical electron radius, is the wavelength, $_e$ is the electron density of the material and $_x$ is the absorption length. The critical angle is given by the relation $_c \quad \sqrt{2}$.

In the region of hard X-rays, the angle is of the order of a few tenths of degree. Below the critical angle, the refractive index is imaginary. Only the so-called evanescent field penetrates into the medium up to the depth of a few nm and the impinging intensity is speculary reflected (Fig. 1, k_{out}). At the same time a wave propagates parallel to the surface. This leads to diffraction on the lattice planes perpendicular to the surface.

The beam is called diffracted-reflected and the diffraction *grazing incidence diffraction* (GIXRD). The take-off angle is similar to the angle of incidence. The GIXRD combines Bragg conditions with total reflection and it is suitable for study of very thin films and surface layers, especially their lateral structure. Penetration depth is significantly reduced with decreasing incidence angle and can be varied over several orders (Fig. 2).

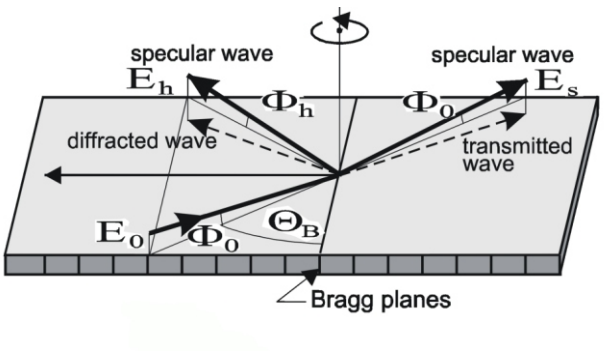

Fig. 1. Geometry of grazing incidence diffraction. (taken from [14]). E_0 ... incident beam, E_s ... specularly reflected beam, E_h ... diffracted-reflected beam.

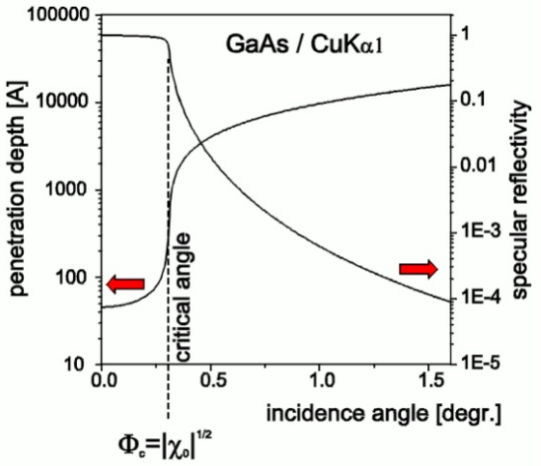

Fig. 2. Penetration depth and reflectivity curve at grazing incidence [14]

The *reflected intensity* is measured as a function of the angle of incidence under specular conditions, e.g at an exit angle of the same value. Then the momentum transfer of elastic scattering is parallel to the surface normal. The value of critical angle is determined by electron density, the decay of the reflectivity curve is related to surface roughness (faster for rough surfaces). It is of special interest for multilayers where two kinds of maxima are observed - Bragg peaks corresponding to the diffraction on multilayer structure and Kiessig maxima between them due to finite thickness of the whole multilayer. Then the total thickness, multilayer period and number of periods can be determined. By simulation, also interface roughness can be studied and it is possible to determine thin film density.

Different scans of diffracted-reflected beam (*GIXRD*) can be realized. This method gives information on the planes perpendicular to the surface. In general, the method provides structural information on the crystalline, diffraction portion of the layer unlike reflectivity giving information on both the 2D-crystalline and amorphous parts of the layer.

Special information on height-height correlations and fluctuations can be obtained by *diffuse scatering* measured at grazing incidence (in nonspecular conditions). In such conditions, lateral structure on mesoscopic length scale can be investigated.

Applications to biological materials

An example of combination of all three scans applied on biological objects is described in [19], where temperature dependent x-ray scattering studies are presented for thin films of purple membranes with the native membrane protein bacteriorhodopsin. The film was highly oriented on Si substrate and this allowed application of all the techniques described above. GIXRD revealed 2D hexagonal lattice formed by the protein within the matrix of the lipid bilayer. The diffraction pattern of the protein -helices does not rely on intermolecular correlations and could be monitored independently of lateral ordering of the proteins. Thermal denaturing transition was studied. A partial unfolding of the helices was observed rather than the complete unfolding process.

Another example also uses highly oriented membrane - phospholipid and antimicrobial peptides [20, 21]. Multilamelar samples were prepared on solid surfaces. By the technique, the short-range order of the lipid chains in the fluid L can be investigated quantitatively. Mean distance between acyl chains and the associated correlation length can be determined. The short-range order in lecithin was found to be severely affected by the amphiphilic peptide magainin 2. Significant disorder in both in the lamellar stacking and the local molecular order in the membrane was found. The chain-chain correlation could be monitored at high precision.

The in-plane and out-of-plane structure of mixed ganglioside-phospholipid monolayers was investigated at the air-water iterface [22]. The surface methods are especially useful for probing the interaction of proteins with monolayers - the effects ranging from protein binding and insertion, fluidization, clustering, and domain formation. Bacterial S-layer protein coupling to lipids was investigated in [23]. Studies of soluble protein monolayers supported by lipid bilayers [24] demonstrated that the equilibrium structure is a sandwich film controlled by tunning the chemical potentials of the lipids and the protein. Different behaviour was observed for high and low concentration of lipid (swelling process or mixed structure with a molecular reorganization).

GIXRD studies of urease films at the air-water interface [25] demonstrated that hexadecylamine, when spread on top of a urease film at the air-water interface, forms a stable, well-organized structure and reflectivity measurements showed that the urease film in the absence of fatty amine molecules unfolds at the interface to a 9Å-thick layer.

A two-dimensional columnar phase in mixtures of DNA complexed with cationic liposomes has been found in the lipid composition [26, 27]. The structure consists of DNA coated by cationic lipid monolayers and arranged on a two-dimensional hexagonal lattice. Two distinct path-

ways from the lamellar to the columnar hexagonal phase of CL/DNA were found.

Reflectivity studies were performed on the mixed Langmuir-Blodgett monolayers of the HIV-1 accesory protein Vpu and the long-chain diacyl phospholipid DLgPC[28]. They were examined as a function of molar ratio at constant surface pressure and as a function of surface pressure at maximal protein/lipid mole ratio.

3.2 X-ray standing waves method [e. g. 16, 29]

There is well-known phenomenon in perfect single crystals - superpositon of incident and diffracted beam generates standing waves. In the region of Bragg diffraction condition, the amplitude of the scattered wave is comparable with the amplitude of the refracted wave and the field intensity is given by the equation

$$I(\vec{r}) \quad \left|\vec{E}_0\right|^2 \; 1 \quad \frac{|\vec{E}_h|^2}{|\vec{E}_0|^2} \quad 2\frac{|\vec{E}_h|}{|\vec{E}_0|}\cos(\vec{h}\vec{r} \qquad) \; ,$$

where $\vec{E}_0$ and $\vec{E}_h$ are the amplitudes of the incoming and diffracted wave, respectively, $\vec{h}$ is the reciprocal lattice vector and is the phase of the $(\vec{E}_h / \vec{E}_0)$ ratio. The intensity has a significant periodic spatial dependence in the direction of the reciprocal lattice vector. The structure of the standing wave is determined by the ratio and the phase . The values of the parameters are changing drastically with the deviation from the Bragg angle. The mutual arrangement of the atomic planes and of the planes of maximum intensity of the wave field is determined by (for = 0, the intensity maxima are on the atomic planes, for = - , the atomic planes coincide with field nodes). In these distinct cases, the interaction of the X-ray wave field with the crystal is significantly different (maximal for = 0). The situation is illustrated in Fig. 3. The intensity of the wavefield at the atomic planes is maximal on the high-angle side of the reflection curve where there is also the strongest interaction of the field with the atoms.

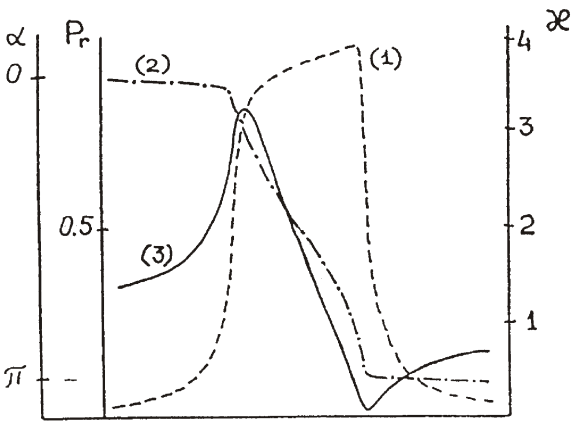

Fig. 3. Schematic picture of the angular dependence (B-) of the reflection coefficient (reflection curve) - 1 (P_R), phase - 2 ( ) and the intensity of the wavefield at the atomic planes - 3 ( ) around the diffraction position [16].

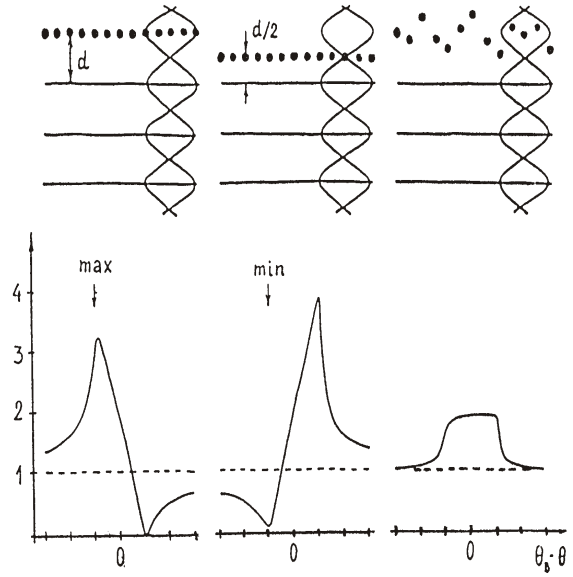

Fig. 4. Illustration of different positions of adsorbed atoms with respect to the antinodes of the XSW field and the corresponding yield of fluorescent radiation of the adsorbed atoms.

We can consider a monolayer of adsorbed atoms on the surface of perfect crystal where the standing waves are generated (Fig. 4). If the adsorbed atoms are located exactly at the position corresponding to the substrate period, related to the generated standing waves, (Fig. 4, left), the fluorescent yield of the adsorbed atoms is identical with the curve (3) of Fig. 3. However, if the adsorbed atoms are displaced only half of the period of standing waves, the fluorescent yield dependence on the diffraction angle is reversed because maximal interaction of the adsorbed atoms with the standing waves is for the case when maxima of the waves fall on the adsorbed atoms (Fig. 4 - middle). It can be seen from the strongly varying curve that it is sensitive even to very small displacement of the layers with a relative experimental accuracy of the order of 1%. Thus, it is possible to detect a displacement of the layer of thousands of the period of the standing wave. This is considerably lower than the wavelength of the incident radiation.

The right part of the figure corresponds to the case of disordered layer. In this case, there is no coherent position of the atoms and equal fractions of the atoms correspond to the nodes and antinodes of the standing waves. The shape of the curve reproduces the reflection curve (Fig. 3, 1).

In general, for partially ordered layers we can determine the so-called *coherent position* - mean plane of the adsorbed atoms with respect to the diffracting planes, and the *coherent fraction* describing the static and dynamic (thermal) displacements of the atoms from the coherent position.

The X-ray standing wave (XSW) method consists in measurement of secondary radiation under the condition of diffraction.- dependence of the yield of secondary radiation on the diffraction angle (Fig. 5). Usually, fluorescent radiation or photoelectrons are detected. The latter have advantage of very small yield depth. In principle, other kind of secondary radiation could also be used (Compton radiation, Auger electrons). Since the fluorescence is element specific process, it is possible to investigate different types of surface atoms separately (marker atoms). This

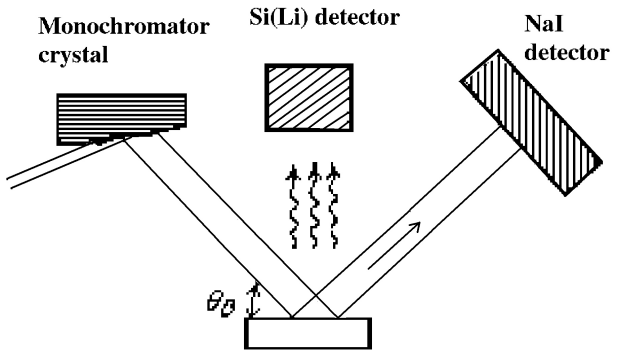

Fig. 5. Experimental arrangement for XSW measurement

chemical selectivity is another goal of the method. Moreover, the energy loss of photolectrons is characteristic of the depth at which the electron was excited and the techniques can be used for depth-resolved studies.

For investigation of organic materials long-period standing waves should be generated (50 - 1000 Å).

The first possibility is to use total reflection from mirror surface. The standing wave is formed as an intereference between incident and specularly reflected waves. The amplitude, phase and the period depends on the incidence angle. At = 0 a standing waves node lies at the mirror surface and the first antinode infinitely far. As the incident angle increases the first antinode moves inward until the critical angle when it coincides with the mirror surface. Advancing above the critical angle, the first antinode remains at the mirror surface while the amplitude of the standing waves dies off rapidly. This method can be called variable-period XSW and it is a powerful tool for studying membrane structure [30]. Typically, measurements are made by scanning in angle and simultaneously monitoring the reflectivity and fluorescence yields from the adsorbed atoms.

The second way is to use the Bragg diffraction from layered synthetic microstructures (alternating low and high electron density materials) with large period [31]. It usually consists of 10-200 layer pairs. Interference of the incident and diffracted beam results in standing wave with the period determined by multilayer d-spacing and the phase varying drastically through narrow Bragg diffraction angular range. Because the angular width of the Bragg peak is on the order of a fraction of miliradian, the period of standing wave remains approximately *fixed* and equal to the d-spacing of the multilayer during the course of a typical XSW measurement.

Application to biological materials

This kind of standing waves is used for study of biomembranes, heavy ion penetration through organic bilayers and multilayers.

A review of membrane structure studies using XSW has been published in [32]. The review discusses membrane structure from the perspective of membrane lipid and protein topology and of the aqueous region close to the membrane surface. XSW is a method capable to give direct structural information with atomic resolution in an element-specific manner on samples that may take the form of isolated membranes or lipid monolayers. Moreover it can be used for both ordered and disordered systems. The method comprises the one-dimensional projection of the spatially averaged in-plane structure along the normal to the supporting solid surface. It can also be used to monitor membrane-related dynamic processes (membrane-lipid phase transitions, ion movement in membrane systems, diffusion). There is a perspective for investigation of protein folding, membrane-protein insertion, surface potential-driven rearrangements in membrane associated ion, lipid, and/or protein distributions and surface binding.

Usually, distribution of marker atom above the substrate is modelled, reflectivity and fluorescence yield calculated and compared to experimental data. Initially, a layered model of refractive index is used. By adjusting the interfacial roughness, reflectivity is fitted and subsequently fluorescence calculated.

LB films are frequently used as models for biomembranes. They also have been studied by the XSW method (zinc atoms distribution in LB trilayer of Zn and Cd arachidate). Membranes up to 1000 Å thick were studied with Å resolution [32].

For investigation of membrane-protein arrangement and behaviour in specific environment, series of lipids and proteins specifically labeled with approapriate marker atoms must be prepared. Because many membrane proteins contain heavy atoms naturally, they are ideal candidates for structural biology studies. These include for example studies of topological relationship of the electron-transfer protein, cytochrome *c*; the biotin-streptavidin complex; protein kinase C; phospholipase A2; bacteriorhodopsin. In [32], the studies of cytochrome *c* bound as a monolayer to a flat supported lipid alayer on an XSW-generating surface is presented. It was shown that the protein retains its globular shape and is hexagonally close-packed while adsorbed at the silver mirror surface.

Recently, also the *in-plane* structure of the biomolecular films (acyl chain ordering) was studied using resonant X-ray beam coupling principle [33]. In this approach, the samples are directly incorporated in the X-ray waveguide [34] created artifically from suitable substrate and a cap layer. The resonantly enhanced diffraction signal can then be measured by tuning the incidence angle to a resonant mode of waveguide.

In conclusion, it can be summarized that recent applications of both traditional (powder diffraction) and rather new (surface scattering) X-ray techniques revealed amazing possibilities for structural studies of biological systems.

References

1. R. B. Von Dreele, "Combined Rietveld and Stereochemical Restraint Refinement of a Protein Crystal Structure," *Journal of Applied Crystallography* **32**, 1084-1089 (1999).
2. R. B. Von Dreele et al, The First Protein Crystal Structure Determination from High-Resolution X-Ray Powder Diffraction Data. A Variant of T3R3 Human Insulin Zinc Complex Produced by Grinding, *Acta Cryst. D* **56** (2000) 1549-1553.

3. J. C. Cockroft, J. Bond, P. Barnes, D. S. Moss, A. J. Basak, J. Wright, 21th European Crystallographic Meeting, Durban, South Africa, August 24-29, 2004, p. 107 (short abstract).
4. J. Wright: Rietveld Structure Refinement of Protein Powder Diffraction Data using GSAS.21th European Crystallographic Meeting, Durban, South Africa, August 24-29, Lecture on Workshop, ref. http://www.ccp14.ac.uk/projects/ecm21-durban/wright/ecm21_wright_gsas_proteins.pdf.
5. L. Dobiášová, R. Kužel, H. Šíchová, Application of powder diffraction in biology? The egg-shell microstructure. *Materials Structure*, **10** (2003), 38-39.
6. C. Meneghini, M. C. Dalconi, S. Nuzzo, S. Mobilio, R. H. Wenk, Rietveld Refinement on X-ray Diffraction Patterns of Bioapatite in Human Fetal Bones, *Biophysical Journal*, **84** (2003) 2021-2029.
7. J. Keckes, I. Burgert, K. Fruhmann, M. Muller, K. Kolln, M. Hamilton, M. Burghammer, S. V. Roth, S. Stanzl-Tschegg, P. Fratzl, Cell-Wall recovery after irreversible deformation of wood, *Nature Materials*, **2** (2003) 810-814.
8. http://www.ccp13.ac.uk
9. T. Kraft, S. Xu, B. Brenner, L. C. Wu, The Effect of Thin Filament Activation on the Attachment of Weak Binding Cross-Bridges: A Two-Dimensional X-Ray Diffraction Study on Single Muscle Fibers, *Biophysical Journal*, **76** (1999) 1494-1513
10. J. Juanhuix, J. Bordas, J. Campmany, A. Svensson, M. L. Bassford, T. Narayanan, Axial Disposition of Myosin Heads in Isometrically Contracting Muscles. C. Meneghini, M. C. Dalconi, S. Nuzzo, S. Mobilio, R. H. Wenk, Rietveld Refinement on X-ray Diffraction Patterns of Bioapatite in Human Fetal Bones, *Biophysical Journal*, **80** (2001) 1429-1441.
12. H. Iwamoto, Y. Nishikawa, J. Wakayma, T. Fujisawa, Direct X-ray Observation of s Single Hexagonal Myofilament Lattice in Native Myofibrils of Striated Muscle. *Biophysical Journal*, **83** (2002) 1074-1081.
13. M. Tolan, X-ray reflectometry - basic principles, *Materials Structure*, **4** (1997), 153-156.
14. S. Stepanov, X-ray reflectometry - basic principles, *Materials Structure*, **4** (1997), 157-163.
15. T. Salditt, Difuse X-ray scattering - An Introduction, *Materials Structure*, **4** (1997), 164-169.
16. M. V. Kovalchuk, A. Yu. Kazimirov, S. I. Zheludeva, Surface-sensitive X-ray diffraction methods: Physics, applications and related X-ray and SR instrumentation, *Materials Structure*, **2** (1995), 3-18.
17. M. Jergel, V. Holý, E. Majková, Thin film studies by X-ray reflectivity and diffuse scattering at grazing incidence. *Materials Structure*, **3** (1996), 101-109.
18. V. Holý, U. Pietsch, T. Baumbach: High resolution X-ray scattering from thin films and multilayers, Springer Tracts in Modern Physics, vol 119, Springer, Berlin, 1999.
19. J. Muller, C. Munster, T. Salditt, Thermal Denaturing of Bacteriorhodopsin by X-ray Scattering from Oriented Purple Membranes, *Biophysical Journal*, **78** (2000) 3208-3217.
20. C. Munster, J. Lu, S. Schinzel, B. Bechinger, T. Salditt, Grazing incidence X-ray diffraction of highly aligned phospholipid membranes containing the antimicrobial peptide magainin 2. *Eur. Biophys. J.* **28** (2000) 683-688.
21. T. Salditt, C. Munster, J. Lu, M. Vogel, W. Fenzl, A. Souvorov, Specular and diffuse scattering of highly aligned phospholipid membranes. *Physical Review E* **60** (1999) 7285-7289.
22. J. Majewski, T. L. Kuhl, K. Kjaer, G. S. Smith, Packing of Ganglioside-Phospholipid Monolayers: An X-Ray Diffraction and Reflectivity Study. *Biophysical Journal*, **81** (2001) 2707-2715.
23. M. Weygand, B. Wetzer, D. Pum, U. B. Sieytr, N. Cuvillier, K. Kjaer, P. B. Howes, M. Lotsche, Bacterial S-Layer Protein Coupling to Lipids: X-Ray and Reflectivity and Grazing Incidence Diffraction Studies. *Biophysical Journal*, **76** (1999) 458-468.
24. V. Petkova, J. J. Benattar, M. Nedyalkov, How to control the molecular architecture of a monolayer of proteins supported by a lipid layer. *Biophysical Journal*, **82** (2002) 541-548.
25. D. Gidalewitz, Z. Huang, S. A. Rice, Urease and Hexadecylamine-Urease Films at the Air-Water Interface: An X-Ray Reflection and Grazing Incidence X-ray Diffraction Study. *Biophysical Journal*, **76** (1999) 2797-2802.
26. I. Koltover, T. Salditt, J. O. Radler, C. R. Safinya, An Inverted Hexagonal Phase of Cationic Liposome - DNA Complexes Related to DNA Release and Delivery. *Science* **281** (1998) 78-81.
27. T. Salditt, I. Koltover, J. O. Radler, C. R. Safinya, Two-dimensional smectic ordering of linear DNA chains in self-assemled DNA-cationic liposome mixtures, *Phys. Rev. Letters*, **79** (1997), 2582-2585.
28. S. Zheng, J. Strzalka, Che Ma, S. J. Opella, B. M. Ocko, J. K. Blasie, Structural Studies of the HIV-1 Accessory Protein Vpu in Lagmuir Monolayers: Synchrotron X-Ray Reflectivity. *Biophysical Journal*, **80** (2001) 1837-1850.
29. R. G. Jones, A. S. Y. Chan, M. G. Roper, M. P. Skegg, I. G. Shuttleworth, C. J. Fischer, G. J. Jackson, J. J. Lee, D. P. Woodruff, N. K. Singh, B. C. C. Cowie, X-Ray Standing Waves at Surfaces. *J. Phys: Condensed Matter* **14** (2002) 4059-4074
30. S. I. Zheludeva, M. V. Kovalchuk, N. N. Novikova, A. N. Sosphenov, X-ray standing waves in LSM for characterization of ultra-thin films. *J. Phys. D*, **26** (1993) A206-A209.
31. R. Zhang, R. Itri, M. Caffrey, Membrane Structure Characterization Using Variable-Period X-Ray Standing Waves. *Biophysical Journal*, **74** (1998) 1924-1936.
32. M. Caffrey, Jin Wang, Membrane-Structure Studies Using X-Ray Standing Waves. *Annu. Rev. Biophys. Biomol. Struct.* **24** (1995) 351-78.
33. F. Pfeiffer, U. Mennicke, T. Salditt, Waveguide-enhanced scattering from thin biomolecular films. *J. Appl. Cryst.* **35** (2002) 163-167.
34. S. Lagomarsino, A. Cedola, S. Di Fonzo, W. Jark, V. Mocella, J. B. Pelka, C. Riekel, Advances in Microdiffraction with X-Ray Waveguide. *Cryst. Res. Technol.* **37** (2002) 758-769.